# Nuclear magnetic resonance: Free-induction decay and spin echoes in a 0.05-T magnetic field

W. Klein
*I. Physikalisches Institut, Universität zu Köln, Zülpicher Strasse 77, 5000 Köln 41, West Germany*

(Received 23 March 1988; accepted for publication 30 March 1989)

NMR-absorption signals in a 2-cm$^3$ sample of glycerol can be observed in a small permanent magnet producing a field of 50 mT. Observing the beat frequency between the marginal oscillator used as spin detector and the Larmor frequency of the spin system after excitation with 10- to 20-$\mu$s high-frequency pulses, the free-induction decay and spin echoes can be detected. The experiment is capable of demonstrating the principles of NMR tomography, e.g., the Carr–Purcell sequence, inversion recovery, and image formation in a field gradient.

## I. INTRODUCTION

Since the discovery of nuclear magnetic resonance (NMR) by Bloch and Purcell and co-workers[1] in 1946, a steadily increasing interest in this field has led to the development of high-resolution NMR techniques for the study of molecular structures, and the investigation of interactions in solids and liquids.

The measurement of transition frequencies in external magnetic fields and the determination of longitudinal and transverse relaxation times have yielded a better understanding of the mechanism of spin–spin and spin–lattice interactions. With the introduction of NMR tomographic image formation,[2] a wide field of applicability in medical research and diagnosis has been opened.

In view of the importance of NMR in physics, chemistry, and medicine, the topic is usually taught in introductory physics courses as well as in advanced laboratory courses. Many experiments demonstrating the principles of NMR have been published.[3,4] Usually, separate experimental setups are applied to study absorption signals and spin echoes.

In this article a versatile low-cost NMR experiment is presented capable of demonstrating resonance transitions, free-induction decay (FID), and spin echoes. As the physical background of NMR has been extensively described in the literature,[5–9] the experimental technique will be emphasized here.

The NMR signals studied with our experimental setup were obtained with a small permanent magnet[10] producing a field of approximately 0.05 T. In similar low fields (0.04 T), even whole-body NMR imaging has been performed.[11]

### A. Absorption signals, free-induction decay, and spin echoes

A 2-cm$^3$ sample of glycerol surrounded by a copper coil is located between the pole faces of a small 0.05-T permanent magnet. The Zeeman splitting of the proton spin states corresponds to a transition frequency of approximately 2 MHz. At room temperature the longitudinal relaxation time will be of the order of 25 ms, and resonance transitions can be observed with repetition frequencies of 10–20 Hz.

Figure 1 shows a block diagram of the apparatus. The magnet is a Newport–Watson magnet[10] consisting of two permanent magnet bars mounted between mild steel plates. The magnetic field in the center of the open space between the pole faces is about 0.05 T with a maximum deviation of 0.1% from the center field value over a volume of $25\times25\times25$ mm$^3$. Modulation coils allow a field modulation of $\pm$ 0.5 mT.

The sample head consists of a glass test tube with an outer diameter of 12 mm. A 14-turn coil of 1.8-mm-diam enameled copper wire and a 4000-pF capacitor constitute the parallel resonance circuit of the spin detector. A 500-pF parallel tuning capacitor is located inside the dectector box. The heart of the spin detector is a low-noise feedback amplifier as developed by Robinson,[12] which includes a demodulation stage.

Figure 2 shows the basic circuit of the Robinson oscillator. With only two minor changes to Robinson's original circuit, the spin detector can also be used for the spin-echo experiments described below. For this purpose the recovery time can be reduced by disconnecting the ground leads of the two $\pi$-filter capacitors preceding the output stage. Two fast diodes connected to the input gate prevent severe overloading of the input circuit by the high-frequency pulse needed for the spin-echo experiments.

Another change in Robinson's original circuit concerns the integrating capacitor. With an additional switch, this capacitor can be changed from 10 $\mu$F to 47 nF for the FID and the spin-echo experiments.

Using a marginal-oscillator-type spin detector provides a number of advantages for the demonstration of spin-echo experiments. The Larmor frequency of the spin system can be directly measured in a cw experiment. Consequently, the frequency of the pulse generator can be set to $\omega_0$ leaving only two more parameters to be adjusted, e.g., the pulse amplitude and pulse duration. Before switching to the pulse mode, the spin detector is slightly detuned so that the

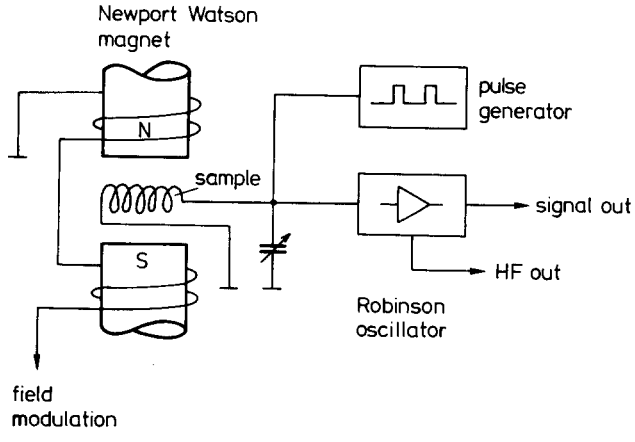


Fig. 1. Block diagram of apparatus.

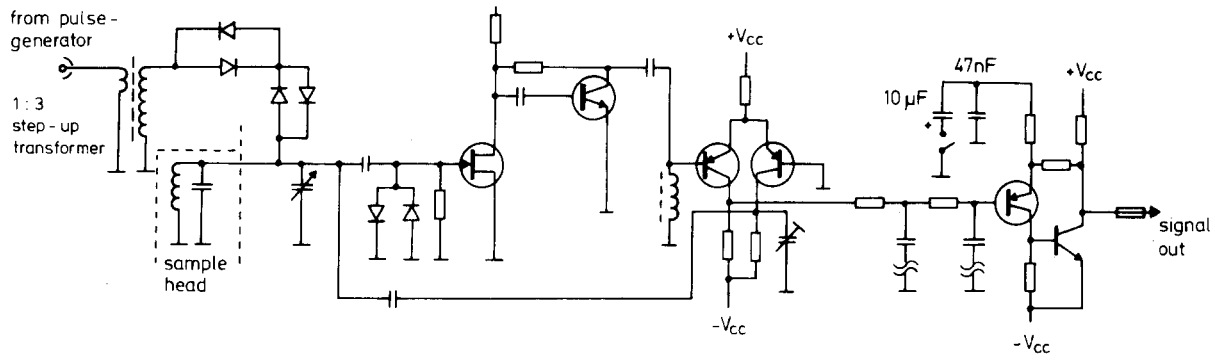


Fig. 2. Basic circuit of the Robinson oscillator. As a variation of Robinson's original circuit, a pair of diodes couples the pulse generator to the sample circuit. Another pair prevents the amplifier input from going into saturation as a result of the large high-frequency pulse applied. The two $\pi$-filter capacitors can be disconnected to reduce the recovery time. A detailed description of the complete circuit can be found in Robinson's paper (Ref. 12).

beat frequency between spin detector and $\omega_0$ can be observed.

Even though the observed signal frequency differs from $\omega_0$, it may serve as a simpler and more direct explanation than the usually measured signal envelopes after demodulation. Furthermore, a moderate sensitivity of the detector can be reached without too much sacrifice in signal-to-noise ratio.

### B. Proton resonance signals

With a 12-Hz modulation of the magnetic field and the tuning capacitor set to the Larmor frequency of protons in the permanent magnet field, the wiggle signal can be observed. In order to obtain a large, slowly decaying signal, the sample coil can be carefully adjusted for optimum field homogeneity.

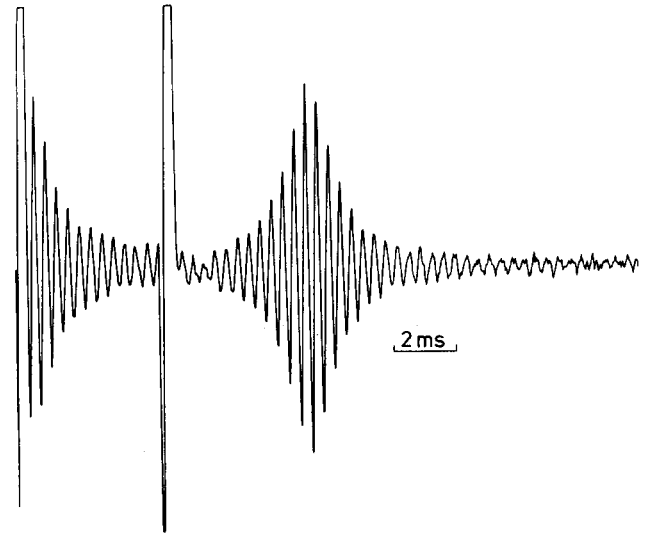


Fig. 3. Spin-echo signals obtained with a 90°–180° pulse sequence. $\Delta H/H \approx 10^{-3}$ across the sample volume.

### C. Free-induction decay

The simplest form of an NMR signal is the FID. Packard and Varian[13] reported a free-induction-decay experiment in the homogeneous Earth magnetic field using 500–1000 $cm^3$ of glycerol. Two similar experiments have been published by Waters and co-workers[14,15] and by Callaghan and Le Gros.[16] These experiments, however, can only be performed in an environment free from magnetic disturbances. In most modern laboratories the field inhomogeneities produced by iron and magnetic fields from power lines severely reduce the observed transverse relaxation times.

The FID can be easily observed in the experiment described here if a 90° pulse with the Larmor frequency is applied to the spin system. In the 0.05-T analyzer field, a 10-$\mu$s pulse with a frequency of about 2.1 MHz and a peak-to-peak voltage of 30 V causes a 90° rotation of the macroscopic magnetization in a time much shorter than the relaxation times involved. The high-frequency pulse is applied to the sample circuit via two parallel diodes. These diodes act as a switch and disconnect the high-frequency pulse generator from the sample circuit at the end of a pulse. A one-to-five step-up transformer matches the low-impedance coaxial cable from the pulse generator to the higher impedance of the sample circuit.

To observe the FID signal, the spin detector is tuned to a frequency differing by a few kilohertz from the transition frequency in the constant 0.05-T field. The pulse generator frequency is set to the Larmor frequency of the spin system that has been determined by the preceding absorption experiment, where the frequency can be measured at the high-frequency output of the Robinson oscillator. After the high-frequency wavetrain, the precessing magnetization produces a beat-frequency signal of a few kilohertz generated by the superposition of the free-induction signal and the voltage of the Robinson oscillator, which has the 47-nF integrating capacitor switched in.

### D. Spin echo

The first spin-echo signal was observed by Hahn[6,17] with a sequence of two 90° pulses. The maximum spin-echo amplitude for a given delay time $\Delta t$ is obtained with a 180°

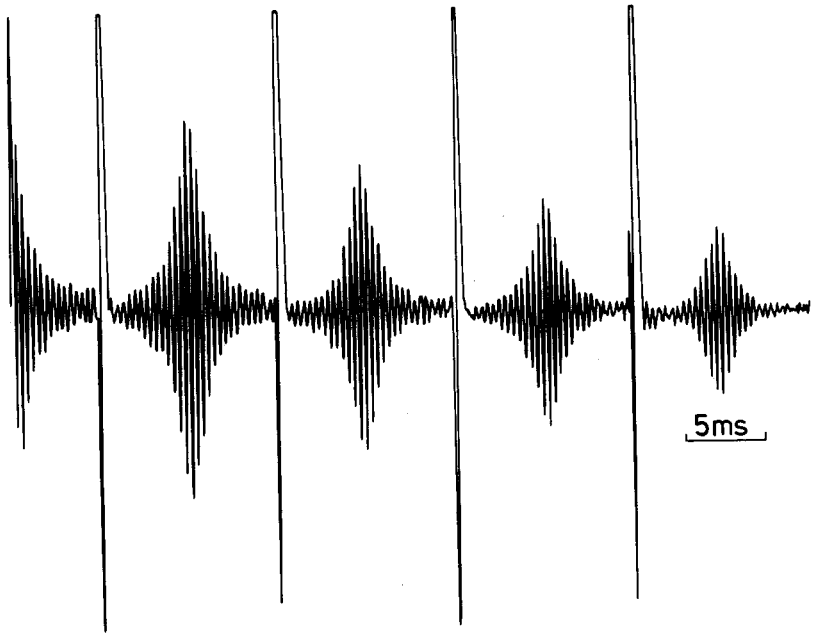


Fig. 4. Carr–Purcell sequence of spin echoes. The 90° pulse is 10 $\mu$s long; the 180° pulses are 20 $\mu$s long.

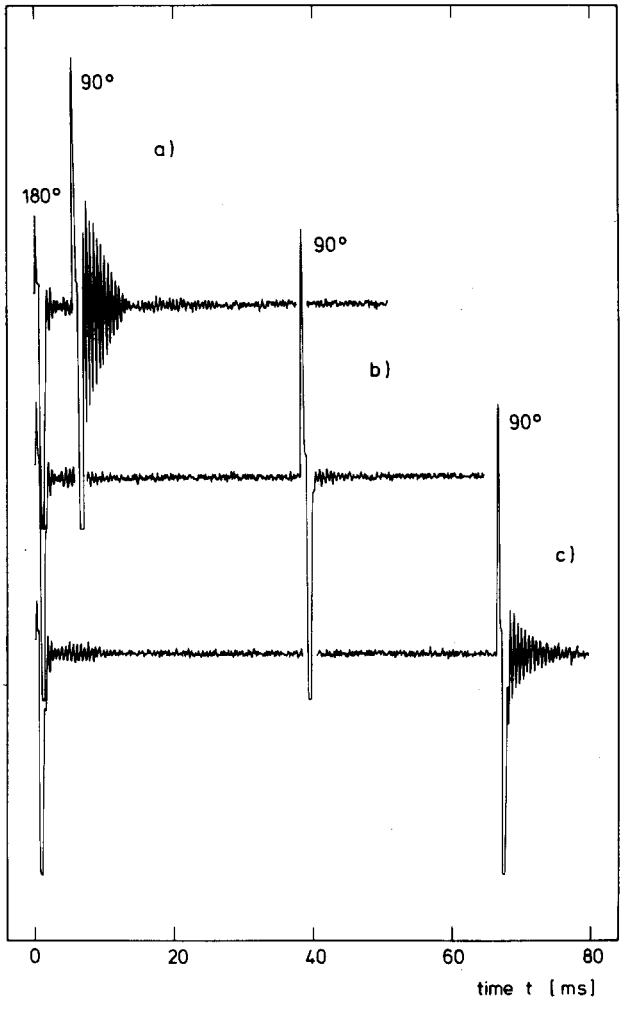


Fig. 5. Inversion recovery signal. Delay time (a) 10 ms, (b) 40 ms, and (c) 75 ms. The first pulse is 20 $\mu$s long; the following pulses are 10 $\mu$s.

pulse following the first 90° pulse. This method is used in NMR tomography to determine the true spin–spin relaxation time $T_2$. The minimum time interval $\Delta t$ for which the spin echo is clearly visible is limited by the relaxation time of FID and Robinson oscillator to about 2 ms. Such a spin echo is shown in Fig. 3. With glycerol the spin echoes can be observed for time intervals up to about 50 ms.

### E. The Carr–Purcell sequence (Ref. 18)

If a 90° pulse is followed by a series of 180° pulses, the series of spin echoes of Fig. 4 appears. The echo amplitude decreases with $\exp(-t/T_2)$, where $T_2$ is the transverse relaxation time of the spin system. With the pulse generator, one to nine 180° pulses can be generated.

In all spin-echo experiments, the duration of the 90° pulse must be chosen to give a maximum FID signal, whereas the second 180° pulse is adjusted for zero FID. Another pulse sequence permits the measurement of the longitudinal relaxation time $T_1$.

### F. Inversion recovery

An initial 180° pulse inverts the magnetization, which recovers at a rate proportional to $[1-2\exp(-t/T_1)]$. No signal is observed until a 90° pulse generates a FID. The FID signal following this second pulse starts with an amplitude proportional to the partially recovered longitudinal magnetization. Hence, by changing the delay time between the inverting 180° pulse and the 90° pulse, $T_1$ can be measured. This inversion recovery signal is reproduced in Fig. 5 for different delay times.

To observe the inversion recovery signal, the frequency of the pulse has to be very close to the Larmor frequency of the protons, and the sample head should be adjusted for maximum field homogeneity to avoid secondary echo signals.

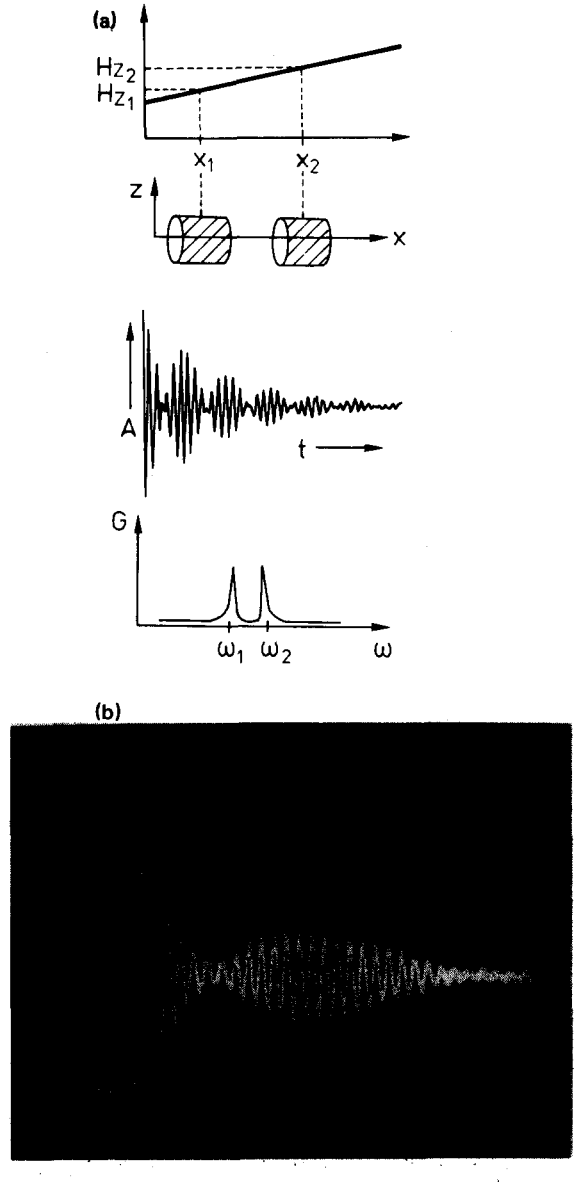


Fig. 6. (a) Signal form and frequency spectrum of a one-dimensional structure subject to a field gradient. Field gradient in $x$ direction. Time and frequency domains are related by Fourier transformations. (b) FID of two 0.1-cm$^3$ glycerol samples spaced 0.5 cm apart in a slightly inhomogeneous region of the field. The signals were averaged over 100 transitions using a Tektronix 7854 oscilloscope.

### G. One-dimensional image formation

The free-induction decay in a homogeneous field consists of a single frequency. If the sample has a structure and is exposed to an additional field gradient, the free-induction decay will contain several frequencies and the frequency spectrum will be related to the geometrical structure via a Fourier transformation. For the simple structure of two separated samples, the field gradient will produce the signal form of Fig. 6(a), and the frequency domain will exhibit two separate frequencies according to the different Zeeman splitting of the energy levels. In NMR tomography the field gradients in space are well defined, and the spatial distribution of proton density and relaxation times can be obtained from either FID or spin echo by means of Fourier transformations.

In our experiment the glycerol sample is separated into two parts with a circular Teflon disk about 6 mm thick. A field gradient along the axis of the sample coil can be easily obtained by moving the sample head toward the edge of the analyzer magnet.

The FID signal of Fig. 6(b) shows the signal modulation caused by sample structure and field gradient. In order to obtain the required resolution, the sample volume has to be reduced to 0.1 cm$^3$. As the signal from such small sample volumes is completely buried in noise, signal averaging must be used. The signals of Fig. 6(b) are an average over 100 FID decays.

## ACKNOWLEDGMENTS

I am indebted to J. Gebhardt for his help with the Robinson oscillator, to P. Paffhausen and his crew for their help with the electronic equipment, to R. Schieder and P. Brunner for many encouraging discussions, to A. Siegert for his advice during the construction of the pulse generator, and to David Jones for reading the manuscript and for helping me to improve my English. I am also glad to thank Th. Becker for the drawings and reproductions and I. M. Pache and L. Eckardt for typing the manuscript. My special thanks goes to Reg Wright for kindly supplying me with detailed information on the Newport–Watson magnet and for his hospitality during the short visit to Oxford Analytics.

[1]Edward M. Purcell, H. C. Torrey, and P. V. Pound, "Resonance absorption by nuclear magnetic moments," Phys. Rev. **69**, 37–38 (1946); Felix Bloch, W. W. Hansen, and Martin Packard, "Nuclear induction," Phys. Rev. B **69**, 127 (1946).

[2]R. C. Gabillard, "Measurement of the relaxation time $T_2$ in the presence of an inhomogeneity in the magnetic field more important than the width of the line," C. R. Acad. Sci. **232**, 1551–1552 (1951); P. C. Lauterbur, "Image formation by induced local interactions: Examples employing nuclear magnetic resonance," Nature **242**, 190–191 (1973); Raymond Damadian, "Tumor detection by nuclear magnetic resonance," Science **171**, 1151–1153 (1971); C. M. Lai and P. C. Lauterbur, "True three-dimensional image reconstruction by nuclear magnetic resonance zeugmatography," Phys. Med. Biol. **26**, 851–886 (1981); A. N. Garroway, P. R. Grannell, and P. Mansfield, "Image formation in NMR by a selective irradiance process," J. Phys. C **7**, L457–L462 (1974); P. Mansfield, "Multi-planar image formation using NMR spin echoes," J. Phys. C **10**, L55–L58 (1977); Waldo S. Hinshaw, "Image formation by nuclear magnetic resonance: The sensitive point method," J. Appl. Phys. **47**, 3709–3721 (1976); Waldo S. Hinshaw, "Spin mapping: The application of moving gradients to NMR," Phys. Lett. A **48**, 87–88 (1974).

[3]Marshall M. Siegel, "Simple demonstration for frequency sweeping, frequency modulation and detecting NMR signals," Am. J. Phys. **43**, 747–748 (1975).

[4]B. H. Muller, J. D. Noble, L. F. Burnett, J. F. Harmon, and D. R. McKay, "Simple spin-echo spectrometer," Am. J. Phys. **42**, 58–64 (1974).

[5]See, e.g., E. R. Andrew, *Nuclear Magnetic Resonance* (Cambridge U.P., Cambridge, UK, 1955).

[6]A. Loesche, "Kerninduktion," *VEB Deutscher Verlag der Wissenschaften*, Berlin, 1957.

[7]R. T. Schumacher, *Introduction to Magnetic Resonance* (Benjamin, New York, 1970).

[8]C. P. Slichter, *Principles of Magnetic Resonance* (Springer-Verlag, NewYork, 1978); A. Carrington and A. D. McLachlan, *Introduction to*

*Magnetic Resonance* (Harper & Row, New York, 1967).
[9]A. Abragam, *Principles of Nuclear Magnetism* (Oxford U. P., Oxford, 1961).
[10]Newport type 03, Newport Instruments Ltd., Blakelands North, Milton Keynes MK1 45AW, England.
[11]J. M. S. Hutchinson, W. A. Edelstein, and G. Johnson, "A whole-body NMR imaging machine," J. Phys. E **13**, 947–955 (1980).
[12]F. N. H. Robinson, A sensitive nuclear quadrupole resonance spectrometer for 2–60 MHz," J. Phys. E **15**, 814–823 (1982).
[13]Martin Packard and Russel Varian, "Free nuclear induction in the Earth's magnetic field," Phys. Rev. **93**, 941 (1954).
[14]G. S. Waters, "A measurement of the Earth's magnetic field by nulcear induction," Nature **176**, 691 (1955).
[15]G. S. Waters and P. D. Francis, "A nuclear magnetometer," J. Sci. Instrum. **35**, 88 (1958).
[16]P. T. Callaghan and M. Le Gros, "Nuclear spins in the Earth's magnetic field," Am. J. Phys. **50**, 709–713 (1982).
[17]E. L. Hahn, "Nuclear induction due to free Larmor precession," Phys. Rev. **77**, 297–298 (1950).
[18]H. Y. Carr and E. M. Purcell, "Effects of diffusion on free precession in nuclear magnetic resonance experiments," Phys. Rev. **94**, 630–638 (1954).

# Tunneling through a truncated harmonic oscillator potential barrier

Jeff D. Chalk
*Physics Department, Southern Methodist University, Dallas, Texas 75275*

(Received 20 April 1988; accepted for publication 18 March 1989)

The sum of a one-dimensional, truncated harmonic oscillator potential and square well of the same range, defined in the positive half-space, serves as a convenient and instructive example for which the Schrödinger equation may have both bound-state and continuum solutions. A superposition of these solutions is used in a study of barrier penetration by a wave packet representing a particle with an initial position in the region of the potential well. The presence or absence of a bound state in the superposition is shown to be the key factor determining the evolution of the wave packet. If no bound state exists, the probability of the particle having a position within the potential well is a monotonically decreasing function of time. If the superposition includes a bound state, however, this probability oscillates slightly because of an interference between the bound-state and continuum components of the wavefunction.

## I. INTRODUCTION

A potential function of rectangular shape is a natural choice for an introduction to the tunneling phenomenon because of the mathematical simplicity provided. The rectangular barrier and square well have been used in discussions of the propagation of a wave packet through a potential.[1–4] In such a discussion, a sequence of "snapshots" of the probability density $|\psi|^2$ provides a very satisfying qualitative view of the evolution of the packet during the tunneling process.

Although the truncated harmonic oscillator potential involves familiar and simple power-series solutions of the Schrödinger equation, it seems that this potential function is overlooked as a useful potential for a pedagogical study of tunneling.[5,6] A sum of truncated harmonic oscillator potential and square well of the same range was used in this article to study the barrier penetration of a wave packet representing a particle with an initial position in the region of the potential well. The investigation was prompted by the author's desire to present to a class in quantum mechanics an interesting alternative to a rectangular potential and an example that emphasizes the continuum solutions.

The potential function considered restricts the motion of a particle of mass $m$ to the half-space $x \geqslant 0$:

$$V(x) = \begin{cases} \infty, & x < 0, \\ -V_0 + \frac{1}{2} m\omega^2 x^2, & 0 < x < a, \\ 0, & x > a. \end{cases} \tag{1}$$

Here, $V_0$ is the maximum potential depth, $a$ is the range, and $\omega$ is the angular frequency. The initial task will be to find bound-state and continuum solutions of the Schrödinger equation. A significant convenience of this potential is the fact that the solutions for the region within the well and in the region of the barrier are one and the same, and can be written down immediately, since they involve the same power series encountered in deriving the solutions for the linear harmonic oscillator. The series is not truncated in this case, however, so that the solutions do not involve Hermite polynomials.

Two sets of potential parameters are considered so as to allow either one or no bound states. Analysis of an assumed initial wavefunction in terms of the two complete sets of energy eigenfunctions will reveal a pronounced difference in the structure of the packets, and the evolution of the packets will differ accordingly. Particular attention is given to the varying probability of the particle having a position within the potential barrier. The results for the two potentials, presented graphically, provide the basis for the final discussion.